ELSEVIER

Journal of Alloys and Compounds 224 (1995) 274–282

Journal of
ALLOYS
AND COMPOUNDS

Gold substitution and superconductivity in $YBa_2Cu_3O_{7-\delta}$:Au

Z. Tomkowicz [a], J. Stanek [a], A. Szytuła [a], A. Bajorek [b], M. Bałanda [b], E. Ściesińska [b], J. Ściesiński [b], M. Guillot [c]

[a] *Institute of Physics, Jagellonian University, Reymonta 4, 30-059 Cracow, Poland*
[b] *The Henryk Niewodniczański Institute of Nuclear Physics, Radzikowskiego 152, 31-342 Cracow, Poland*
[c] *Service National des Champs Intenses, C.N.R.S., 38042 Grenoble, France*

Received 15 November 1994; in final form 9 January 1995

Abstract

The samples of nominal compositions $(Y_{1-x}Au_x)Ba_2Cu_3O_{7-\delta}$, $Y(Ba_{0.96}Au_{0.04})_2Cu_3O_{7-\delta}$, $YBa_2(Cu_{0.97}Au_{0.03})_3O_{7-\delta}$ and $YBa_2Cu_3Au_{0.087}O_{7-\delta}$ were synthesized and comparative studies were performed by means of X-ray diffraction, ^{197}Au Mössbauer effect, electrical resistance, a.c. and d.c. magnetometric and far infrared absorption methods. The $(Y_{1-x}Au_x)Ba_2Cu_3O_{7-\delta}$ and, particularly, $(Y_{0.95}Au_{0.05})Ba_2Cu_3O_{7-\delta}$ sample showed better homogeneity and sharper transition to the superconducting state than its $YBa_2(Cu_{0.97}Au_{0.03})_3O_{7-\delta}$ counterpart. It is concluded that Au substitutes for Cu(1) in chain positions while excess Cu atoms enter other, probably Y, lattice positions contributing to an observed paramagnetism. The solubility limit of Au in the chain positions was determined to be $x=0.08$.

Keywords: Gold substitution; Superconductivity

1. Introduction

Gold is the only known dopant to $YBa_2Cu_3O_{7-\delta}$ which increases critical temperature T_c of transition to the superconducting state. The role of silver is controversial in this respect [1] although it is known that silver improves some superconducting properties. The initial interest in gold substitution was to study an influence of Au crucible used to grow single crystals of $YBa_2Cu_3O_{7-\delta}$. In the extensive paper Cieplak et al. [2] stated a favourable effect of gold on the superconducting properties of $YBa_2Cu_3O_{7-\delta}$: the sharp transition to the superconducting state and T_c enhanced by about 1.5 K. It has been established that Au substituted for the Cu(1) chain site and had a valence 3+ in agreement with other reports. The determined solubility limit was about 10 at.% of the chain copper. Eibschütz et al. [3] observed by ^{197}Au Mössbauer effect that gold valence changes as a function of oxygen stoichiometry from 3+ at full oxygenation to 1+ for deoxygenated compound. It was suggested by Tallon et al. [4] that T_c enhancement is caused simply by a reduction of hole concentration to the optimum at $T_{c\,max}$, because pure $YBa_2Cu_3O_7$ ($\delta=0$) is overdopped. But while some authors state increase in oxygen stoichiometry with gold doping, others conclude the inverse. Recently a paper of Veretnik and Reich [5] has appeared where the authors report $T_c=97$ K for their melt-textured $YBa_2Cu_3O_{7-\delta}$:Au with gold diffused from a film of sputtered gold covering the sample. A decrease in oxygen stoichiometry was stated by means of Auger electron spectroscopy and shortening of the *c*-axis was observed, contrary to all previous reports. It is seen in the light of the above facts that preparation conditions can be essential for superconducting properties of gold substituted $YBa_2Cu_3O_{7-\delta}$.

If gold really substitutes for Cu(1) a question arises as to why Au^{3+}-ion behaves differently to other trivalent dopants. For example, Co^{3+}- and Fe^{3+}-ions induce an orthorhombic to tetragonal structural deformation at a concentration of about 3–5 at.% and decrease T_c considerably. Gold substitution, instead, has a little effect on orthorhombic distortion and increases T_c slightly [2]. It seems natural that heavy Au-ions should affect the lattice dynamics. The effect of Au on some Raman modes has been discussed extensively [6]. However, the results can not be interpreted unambiguously. Therefore we recognize that it is interesting to measure, among other things, far infrared absorption spectra in order to see how infrared modes behave on gold substitution.

SSDI 0925-8388(95)01546-9

In this paper we report the results of our comparative studies by different methods for $YBa_2Cu_3O_{7-\delta}$:Au samples where gold was intended to substitute for Y, Ba and Cu in turn and also used as an additive. In this way, we hope, more certain conclusions can be set about gold influence on the superconductivity mechanism. We also look at what is unusual in gold substitution for Y since we observed in our earlier study a considerable (but non reproducible) enhancement of T_c for such substitution. The paper is organized in the following way. In Section 2 a description of sample preparation and experimental methods is given. In the first part of Section 3 a structural characterization by X-ray diffraction and ^{197}Au Mössbauer effect is given. Later, the results of electrical resistance measurements are given followed by characterization by magnetic methods. At the end we present far infrared absorption spectra. The last part is devoted to the discussion of a problem of eventual impurities and of gold influence on magnetic properties of $YBa_2Cu_3O_{7-\delta}$:Au.

2. Experimental

The following nominal compositions were prepared: $(Y_{1-x}Au_x)Ba_2Cu_3O_{7-\delta}$ with $x=0.03$, 0.05, 0.08, 0.10, 0.15, $Y(Ba_{0.96}Au_{0.04})_2Cu_3O_{7-\delta}$, $YBa_2(Cu_{0.97}Au_{0.03})_3O_{7-\delta}$ and $YBa_2Cu_3Au_{0.087}O_{7-\delta}$. Additionally the sample with Ag $(Y_{0.95}Ag_{0.05})Ba_2Cu_3O_{7-\delta}$ was prepared for comparative purpose. The samples were prepared by the usual ceramic method from high purity oxides and $BaCO_3$. The special reason for using Au_2O_3 was that this material is accessible in the fine powder form which is essential for obtaining a very homogeneous sample. The powders were thoroughly mixed and hand pressed into pellets, which were next calcined in an alumina boat in air at 900 °C. Then the samples were crushed, pressed with the force of 3 tons into pellets of 10 mm diameter and thickness ≈ 2 mm and sintered at 900 °C under flowing oxygen for 24 h and then cooled with a rate of 2 °C min^{-1} still under flowing oxygen. This process was repeated two times, but the temperature of sintering was increased to 940 °C. We also tried to sinter the samples on a gold foil but the quality of the obtained samples was worse. The samples stuck to the foil and turned green in the area of contact with gold.

For some measurements the samples were deoxygenated by annealing for 3 h at 600 °C under flowing argon.

X-ray diffraction was used for checking the quality of the samples and for determination of the lattice constants.

The ^{197}Au Mössbauer spectra were recorded in a helium bath cryostat with the source and absorber at 4.2 K. The ^{197}Pt source with an initial activity of 200 mCi was used. The velocity scale was calibrated with a ^{57}Fe spectrum of metallic iron.

The samples were next characterized by different methods. Electrical resistance $R(T)$ measurements were carried out by the four point method with reversing d.c. current. The samples were in the form of parallelepipeds with approximate dimensions $1.5\times2\times10$ mm^3. Contacts were made by soldering with an In:Au alloy. An APD refrigerator with helium exchange gas cryostat was used for cooling the samples. The cryostat was equipped with a high accuracy temperature controller.

A.c. magnetic susceptibility χ_{ac} measurements were carried out by the mutual inductance method at frequency 122 Hz of alternating magnetic field H_{exc} using a glass cryostat. A mutual inductance bridge of a design of Gotszalk and Lisowski [7] was used. Both components χ' and χ'' of the complex susceptibility were measured as a function of temperature and amplitude of H_{exc}. The samples were not screened from the earth magnetic field.

D.c. magnetic measurements were carried out by means of a Faraday type balance. The samples for measurement were powdered and loosely packed in a container. After cooling the samples in zero magnetic field the measurements were performed with increasing temperature.

High field magnetization measurements for selected samples were performed at C.N.R.S. by means of the extraction magnetometer described in Ref. [8]. The samples were cooled in zero magnetic field. Halves of the total hysteresis loops for samples in the form of pressed powder cylinders of 5 mm diameter were registered in the applied field up to 200 kOe. Field steps were equal 2, 4 and 5 kOe with the field variation speed of 0.1 or 1 kOe s^{-1}.

Room temperature infrared absorption measurements were made in the 100–650 cm^{-1} wavenumber range using a Digilab FTS-14 Fourier transform spectrometer set at 2 cm^{-1} resolution. A sample cell of 20 mm in diameter with polyethylene windows was used. Samples were prepared from ≈ 20 mg of the manually ground superconductor mixed with Apiezon L grease. The same sample cell filled only with Apiezon was used as a reference.

3. Results and discussion

All the samples doped with not too much gold showed high quality X-ray diffraction patterns. Samples $(Y_{1-x}Au_x)Ba_2Cu_3O_{7-\delta}$ were rentgenographically pure up to $x=0.08$. The sample $(Y_{0.90}Au_{0.10})Ba_2Cu_3O_{7-\delta}$ showed small impurity peaks probably coming from $BaCuO_2$ and CuO. No peaks from metallic gold were seen. The sample $(Y_{0.85}Au_{0.15})Ba_2Cu_3O_{7-\delta}$ showed large contaminations (also with metallic gold). For comparison the $(Y_{0.95}Ag_{0.05})Ba_2Cu_3O_{7-\delta}$ sample, besides more pronounced $BaCuO_2$ peaks, showed also a remarkable CuO peak. A small peak from CuO was also observed for $Y(Ba_{0.96}Au_{0.04})_2Cu_3O_{7-\delta}$. The pellets of gold substituted samples showed remarkable preferred orientation of grains such that their *ab* planes were nearly parallel to the pellet plane.

The lattice constants for $(Y_{1-x}Au_x)Ba_2Cu_3O_{7-\delta}$ samples were determined using the least squares method. The results are presented in Table 1. The lattice constants *a* and *b* are unchanged but *c* increases with gold doping. This is in full agreement with the literature [2,9] and points out that gold enters into the crystal structure.

In order to answer the question as to what the gold location is in the lattice, the Mössbauer effect measurements were carried out. The ^{197}Au Mössbauer spectra obtained at liquid helium temperature are shown in Fig. 1 for as-obtained and for deoxygenated gold doped samples. The spectra were fitted assuming lorentzian line shape. Such a simplified numerical approach is allowed by a small effective absorber thickness $t_a \approx 1$ of our samples containing only about 30 mg Au cm^{-2}. The hyperfine parameters: isomer shift IS and quadrupole splitting QS are given in Table 2. Component of metallic gold is characterized by a single line with QS = 0. As it is seen the metallic gold component is present only for $Y(Ba_{0.96}Au_{0.04})_2Cu_3O_{7-\delta}$ and $YBa_2(Cu_{0.97}Au_{0.03})_3O_{7-\delta}$ samples, but $(Y_{0.95}Au_{0.05})Ba_2Cu_3O_{7-\delta}$ sample shows only one component characteristic by its IS and QS values for Au^{3+}. After deoxygenation this component is transformed to that characteristic for Au^{1+}. It is known from coordination chemistry that the coordination of Au^{3+} can be only plane-square and the coordination of Au^{1+} only linear. Taking this into account together with the valence change of gold after deoxygenation one concludes simply that gold is located in chain positions. This conclusion agrees with the results of Eibschütz et al. [3]. However, due to our way of synthesis we succeeded in obtaining more homogeneous samples. The spectra of Eibschütz et al. were dominated by a big component from metallic gold. The lack of metallic gold component for the $(Y_{0.95}Au_{0.05})Ba_2Cu_3O_{7-\delta}$ sample witnesses that all the gold was incorporated into the structure for this sample. However, in the Mössbauer spectrum of $(Y_{0.90}Au_{0.10})Ba_2Cu_3O_{7-\delta}$ the fraction of metallic gold is 18% (see Table 2). It follows from this fact that the solubility limit of gold in chain positions is 8%. This is in good agreement with the result of Welp et al. [10] obtained by neutron activation analysis for a single crystal of $YBa_2Cu_3O_{7-\delta}$ grown in a gold crucible.

Table 1
Lattice constants for $(Y_{1-x}Au_x)Ba_2Cu_3O_{7-\delta}$. The errors in parentheses are standard deviations

x	*a* (Å)	*b* (Å)	*c* (Å)
0.03	3.881 (1)	3.815 (1)	11.674 (3)
0.05	3.880 (1)	3.815 (1)	11.682 (3)
0.08	3.881 (1)	3.815 (1)	11.693 (3)

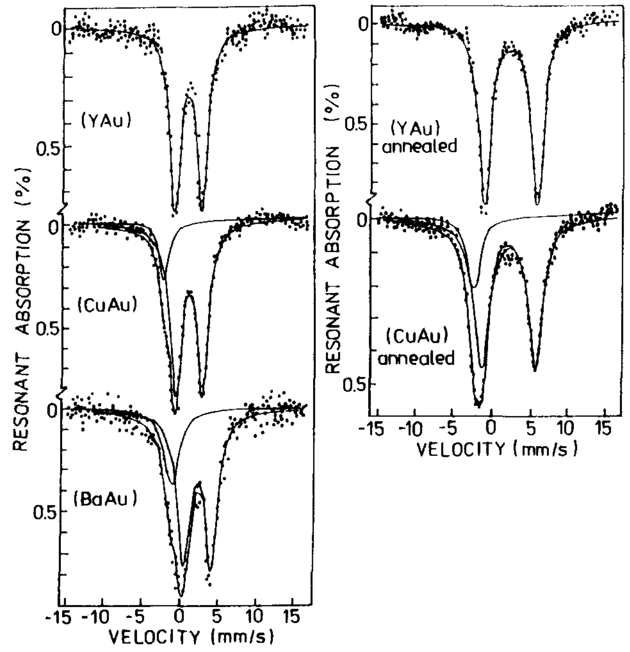

Fig. 1. Mössbauer spectra at 4.2 K for as-obtained and deoxygenated (annealed) gold doped samples. (YAu) means $(Y_{0.95}Au_{0.05})Ba_2Cu_3O_{7-\delta}$; (CuAu), $YBa_2(Cu_{0.97}Au_{0.03})_3O_{7-\delta}$; (BaAu), $Y(Ba_{0.96}Au_{0.04})_2Cu_3O_{7-\delta}$. Solid lines are results of the fitting procedure. Small single line component comes from metallic gold.

The superconducting and normal state properties of samples were characterized by electrical resistance and magnetic methods.

Table 3 summarizes results of the $R(T)$ measurements giving the values of T_c, width of transition ΔT_c and the slope of *R* vs. *T* dependence in the normal state. The highest T_c, the most sharp transition and maximum slope were observed for $(Y_{0.95}Au_{0.05})Ba_2Cu_3O_{7-\delta}$. Summary $R(T)$ and $\chi_{ac}(T)$ characteristics of transition for $(Y_{0.95}Au_{0.05})Ba_2Cu_3O_{7-\delta}$ are shown in Fig. 2. In addition, dR/dT and $d\chi'_{ac}/dT$ curves are also shown. The latter exhibits a double peak structure in accordance with the presence of two steep regions of χ' curve. The general appearance and relative placements of all characteristics prove good homogeneity of the sample.

Our $R(T)$ dependence, although obtained for a polycrystalline sample, is characteristic for the resistance in the *ab* plane because of the known fact that the resistance in this plane is much lower than along the *c*-axis and because of the above mentioned preferred orientation of the grains.

The very good quality of $(Y_{0.95}Au_{0.05})Ba_2Cu_3O_{7-\delta}$ samples stimulated us to determine the dimensionality

Table 2
^{197}Au Mössbauer hyperfine interaction parameters of gold substituted samples: A, marks deoxygenated sample; IS, isomer shift relative to ^{197}Au in Pt; QS, quadrupole splitting; *W*, full width at half maximum; *f*, area under line which accounts for a part of a given component. The errors in parentheses are standard deviations

Sample	IS (mm s^{-1})	QS (mm s^{-1})	W (mm s^{-1})	f (%)
$(Y_{0.95}Au_{0.05})Ba_2Cu_3O_{7-\delta}$	2.10 (1)	3.52 (3)	1.8 (2)	100 (3)
$(Y_{0.95}Au_{0.05})Ba_2Cu_3O_{7-\delta}$A	3.40 (1)	6.89 (2)	1.9 (1)	100 (3)
$(Y_{0.90}Au_{0.10})Ba_2Cu_3O_{7-\delta}$	2.17 (4)	3.55 (7)	2.0 (2)	82 (5)
	−1.04 (11)	0	2.0 (3)	18 (5)
$YBa_2(Cu_{0.97}Au_{0.03})_3O_{7-\delta}$	2.04 (1)	3.55 (2)	1.8 (1)	88 (3)
	−1.18 (4)	0	1.8 (2)	12 (3)
$YBa_2(Cu_{0.97}Au_{0.03})_3O_{7-\delta}$A	3.41 (2)	7.11 (4)	2.0 (1)	83 (3)
	−1.17 (4)	0	1.8 (2)	17 (3)
$Y(Ba_{0.96}Au_{0.04})_2Cu_3O_{7-\delta}$	2.09 (2)	3.62 (4)	2.1 (1)	76 (5)
	−1.36 (6)	0	2.5 (2)	24 (5)

Table 3
Results of electric resistance measurements for gold doped $YBa_2Cu_3O_{7-\delta}$ samples: T_c, superconducting critical temperature (midpoint); ΔT_c, transition width (5–95% of resistance change at transition); slope, relation of resistance at 300 K to that measured at 105 K

Sample	T_c (K)	ΔT_c (K)	Slope
$YBa_2Cu_3O_{7-\delta}$	92.0	1.2	2.05
$YBa_2Cu_3Au_{0.087}O_{7-\delta}$	91.6	1.2	1.77
$Y(Ba_{0.96}Au_{0.04})_2Cu_3O_{7-\delta}$	91.7	1.2	1.70
$YBa_2(Cu_{0.97}Au_{0.03})_3O_{7-\delta}$	91.2	1.6	1.27
$(Y_{0.95}Au_{0.05})Ba_2Cu_3O_{7-\delta}$	92.3	0.6	2.21
$(Y_{0.92}Au_{0.08})Ba_2Cu_3O_{7-\delta}$	92.0	1.0	1.94
$(Y_{0.90}Au_{0.10})Ba_2Cu_3O_{7-\delta}$	92.1	2.7	2.03

of the fluctuation excess conductivity. Although many papers were devoted to the fluctuation conductivity still there are some controversies. Besides, the influence of different admixtures on dimensionality was not studied.

The contribution of excess conductivity can be best shown by differentiation of the $R(T)$ curve. It is seen in Fig. 3 that fluctuations are present below 170 K where the dR/dT curve diverges from a straight line. The slope of this line is different from zero which proves that the $R(T)$ dependence in a normal state at the high temperature region is of parabolic form rather than of $aT+b/T$ form as given by Anderson and Zou [11].

The excess conductivity $\Delta\sigma$ vs. $\epsilon=(T-T_c)/T_c$ dependence in a double logarithmic scale is shown in Fig. 4 (T_c was taken at the maximum of dR/dT). No temperature region with $\gamma=1/2$ or $\gamma=1$ was observed, where γ is the exponent in the Aslamazov–Larkin [12] expression $\Delta\sigma=A\epsilon^{-\gamma}$. The value of the index γ as determined from the slope of the approximately linear part in Fig. 4 equals 0.6 ± 0.02, when the parabolic form of $R(T)$ in the normal state was assumed. When the Anderson and Zou formula for $R(T)$ was assumed, $\gamma=0.45$ was obtained with the factor A about 2 times greater. Similar results: $\gamma=0.65$ and $\gamma=0.3$ respectively, were obtained by Fontana et al. [13] for $YBa_2Cu_3O_{7-\delta}$.

Recently Gauzzi [14] generalized the Aslamazov–Larkin theory to the short coherence length superconductors. Our $\Delta\sigma$ vs. ϵ curve in Fig. 4 can be even better described by this new theory for the 3D case (in particular, the small inflection near $\epsilon=0.02$ has been also reproduced). This points to the three-dimensionality of superconducting fluctuations in gold substituted $YBa_2Cu_3O_{7-\delta}$.

A.c. susceptibility χ' and χ'' vs. temperature curves are shown in Fig. 5(a) for different amplitudes of exciting magnetic field H_{exc}. For $H_{exc}=0.02$ Oe and 0.06 Oe only one, i.e. intergrain, peak of χ'' is seen. For greater H_{exc} a second smaller (intragrain) χ'' peak located near T_c appears.

Positions of both inter- and intra-grain peaks on the temperature scale were drawn as a function of H_{exc}, see Fig. 5(b). According to the Bean model [15] (taking into account the sample shape) the value of intergrain critical current J_c can be determined. The extrapolated value of J_c at the temperature of liquid nitrogen, obtained from Fig. 5(b) is about 160 A cm^{-2}, so a little more than for undoped $YBa_2Cu_3O_{7-\delta}$ prepared in a similar way. The position of the intragrain peak is nearly constant for different H_{exc}. This suggests that intragrain critical current of single grains is many orders of magnitude greater than the intergrain one.

In order to determine intragrain critical current magnetic hysteresis loops were measured at 4.2 K in a magnetic field up to 200 kOe. Also the $YBa_2Cu_3O_{7-\delta}$ sample was measured for comparison. The loops are shown in Fig. 6. It is seen that the width of the loop

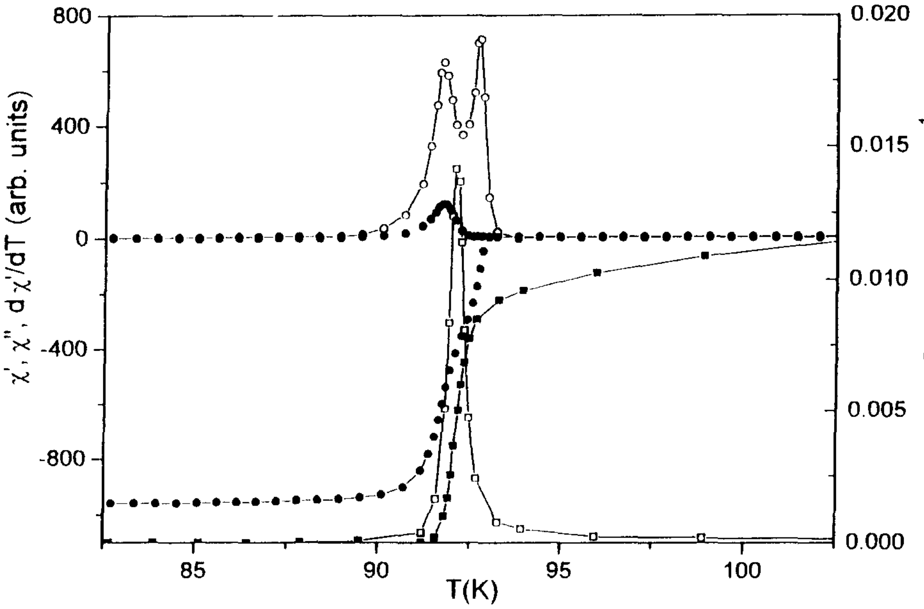

Fig. 2. A.c. magnetic susceptibility and electrical resistance vs. temperature near T_c for $(Y_{0.95}Au_{0.05})Ba_2Cu_3O_{7-\delta}$. Black circles, χ' (lower curve) and χ'' (upper curve); black squares, R; open circles (double peak), $d\chi'/dT$; open squares, dR/dT.

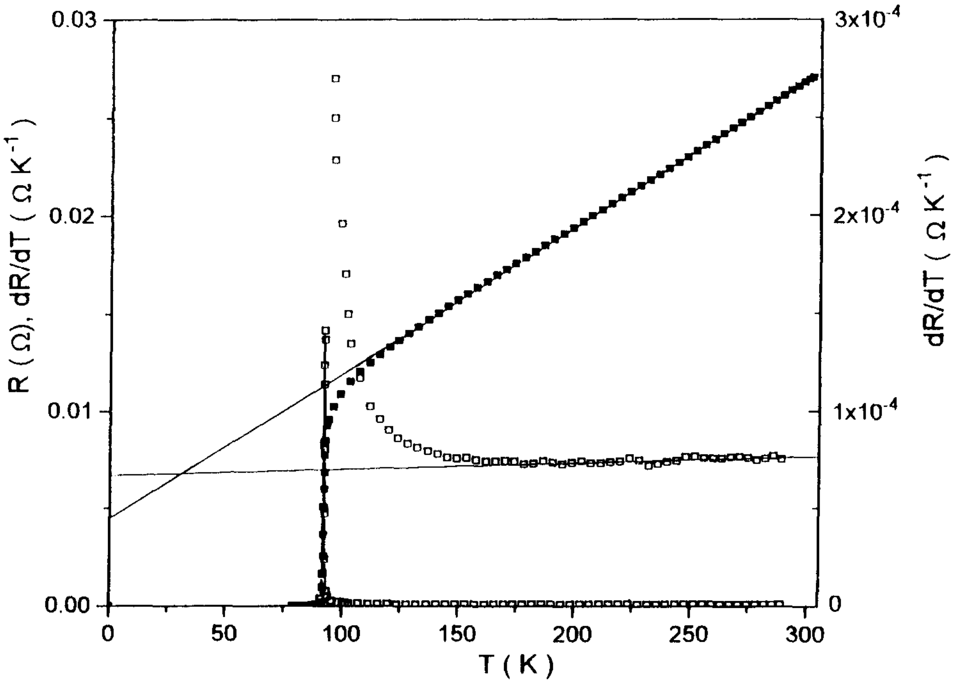

Fig. 3. Temperature dependencies of electrical resistance: black squares and dR/dT; open squares for $(Y_{0.95}Au_{0.05})Ba_2Cu_3O_{7-\delta}$. Also right side of dR/dT magnified 100 times is shown.

is a bit lower for gold doped samples than for the $YBa_2Cu_3O_{7-\delta}$ sample. The width of the loop, according to the Bean model, is a measure of intragrain critical current, provided a grain diameter is known. It was proved by means of scanning electron microscope that grain diameters for our gold doped and $YBa_2Cu_3O_{7-\delta}$ samples (as-obtained i.e. before powdering for measurements) were of comparable magnitude about ≈ 10 μm. So, a smaller width of loop at least for $(Y_{0.95}Au_{0.05})Ba_2Cu_3O_{7-\delta}$ seems to agree with better perfection of this sample which should have fewer pinning centres.

It is seen from Fig. 6 that some paramagnetic contribution is superimposed over the hysteresis loops. This contribution increases with the gold concentration. Its value was calculated taking $(M^+ + M^-)/2$, where M^+ and M^- were the values of magnetizations from the upper and lower loop branch respectively. The values obtained in this way are correct only for the highest magnetic fields. Fig. 7 presents the magnetic field

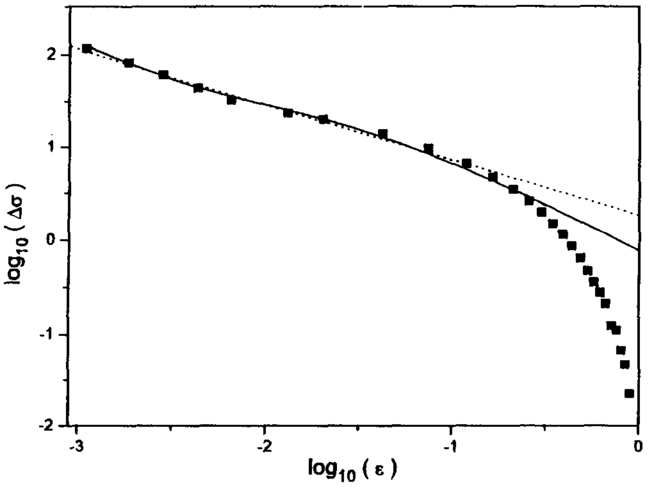

Fig. 4. Fluctuation conductivity (σ in Ω^{-1}) vs. reduced temperature dependence plotted in double logarithmic scale for $(Y_{0.95}Au_{0.05})Ba_2Cu_3O_{7-\delta}$. Dotted line is a linear fit, solid line is a fit according to Gauzzi's theory [14].

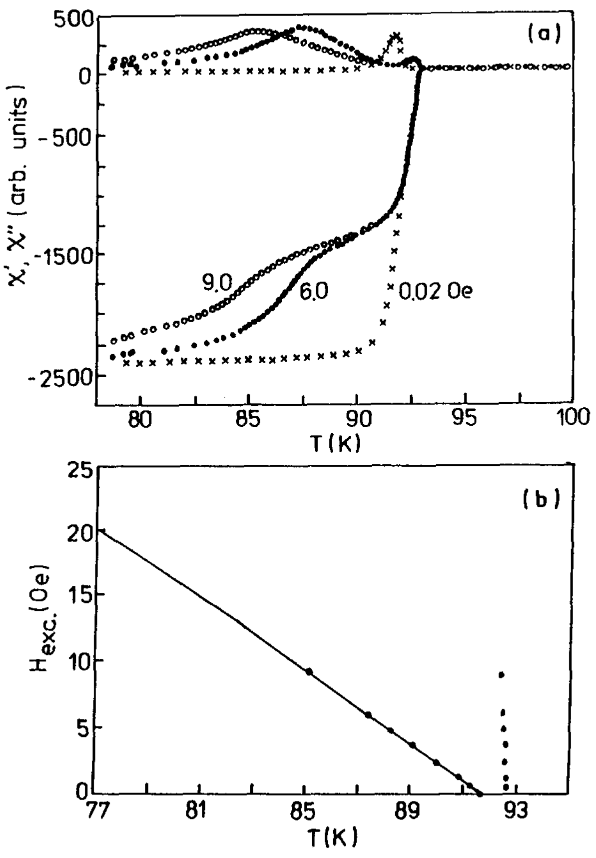

Fig. 5. (a) Temperature dependencies of χ' (lower curves) and χ'' (upper curves) for selected values of the amplitude of exciting magnetic field H_{exc} obtained for the sample $(Y_{0.95}Au_{0.05})Ba_2Cu_3O_{7-\delta}$ (b) Temperature position of χ'' inter- and intra-grain peak drawn as a function of H_{exc}.

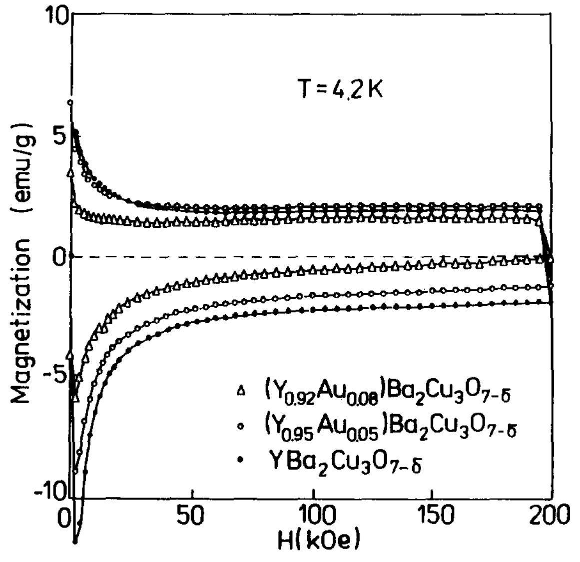

Fig. 6. Magnetization loops.

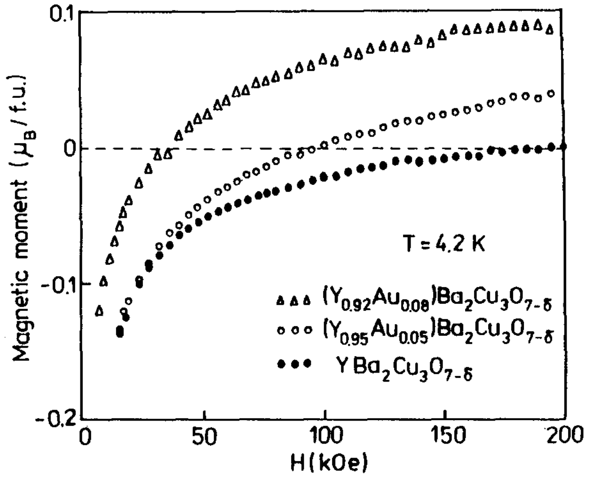

Fig. 7. Magnetic field dependence of magnetic moment per formula unit as derived from Fig. 6.

dependence of the paramagnetic contribution expressed as the number of Bohr magnetons per formula unit. It is seen that this number at 200 kOe is nearly equal to the gold concentration x, as if each incorporated gold ion contributed 1 μ_B of magnetic moment.

In Fig. 8 d.c. magnetic susceptibility vs. temperature dependencies are compared for the superconducting state. It is seen that the screening effect is greater for Y substituted samples and particularly for $(Y_{0.95}Au_{0.05})Ba_2Cu_3O_{7-\delta}$, but it is the lowest for $YBa_2(Cu_{0.97}Au_{0.03})_3O_{7-\delta}$. So, the first critical magnetic field H_{c1} is greater for Y substituted samples. From magnetization vs. magnetic field H dependence measured for $(Y_{0.95}Au_{0.05})Ba_2Cu_3O_{7-\delta}$ in low H at 4.2 K the value of H_{c1} was estimated to be about 200 Oe.

The separate d.c. magnetic measurements were carried out for superconducting and deoxygenated non-superconducting gold doped samples. Temperature dependencies of magnetic susceptibility of gold doped superconducting samples in normal state and of deoxygenated samples are compared in Fig. 9. The slope

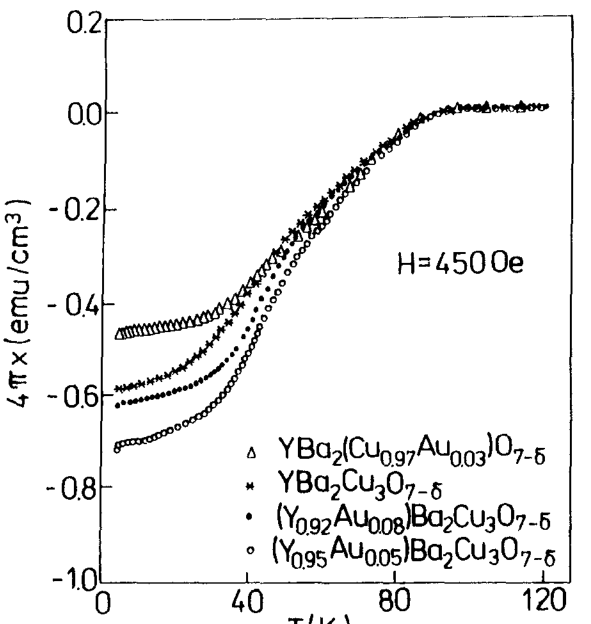

Fig. 8. Comparison of temperature dependencies of magnetic volume susceptibilities in superconducting state.

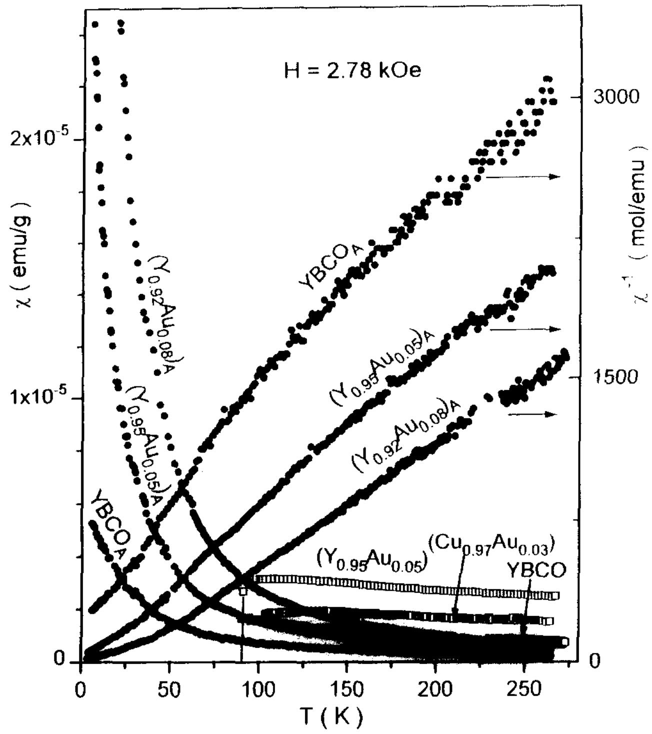

Fig. 9. Temperature dependencies of magnetic susceptibility for oxygenated and deoxygenated samples. Reciprocal molar susceptibility for deoxygenated samples is also shown. Subscript A denotes a deoxygenated sample.

$d\chi/dT$ for superconducting samples is negative. According to Triscone et al. [16] it is characteristic for overdopped (with holes carriers) samples having $\delta=7$. The oxygen diffusion in gold doped samples is much higher than in undoped samples [17], so it is easier for them to saturate with oxygen. On the other hand, this negative slope can be also caused by a presence of some paramagnetic impurities, which can also slur the rounding near T_c arising from the fluctuation diamagnetism. However, this rounding is clearly present for $x=0.05$ and $YBa_2(Cu_{0.97}Au_{0.03})_3O_{7-\delta}$ although the samples were powdered for measurements. Our nonsubstituted samples prepared in a similar way are not of so good quality so the rounding is not observed in this case. It is also seen that χ for superconducting samples in normal state i.e. above T_c increases with gold doping. After deoxygenation the susceptibility drops in this temperature range, but still is an increasing function of gold concentration. The deoxygenated samples show paramagnetic behaviour.

The temperature dependencies of χ for deoxygenated samples were analyzed according to the formula

$$\chi=\chi_0+\frac{C}{T-\theta}$$

where χ_0 is independent of the temperature part, and

$$C=\frac{N_A\mu_B^2}{3k}\,p_{\text{eff}}^2$$

All notations are standard. This formula describes correctly experimental results only above some rather well determined temperature T_p which is ≈ 25 K for $YBa_2Cu_3O_{7-\delta}$, ≈ 40 K for $(Y_{0.95}Au_{0.05})Ba_2Cu_3O_{7-\delta}$ and ≈ 60 K for $(Y_{0.92}Au_{0.08})Ba_2Cu_3O_{7-\delta}$. Below T_p magnetic correlations cause remarkable deviation from the paramagnetic behaviour as can be seen from the temperature dependence of $(\chi T)^{1/2}$. From fits, effective magnetic moments p_{eff} per unit cell and paramagnetic Curie temperatures θ were obtained. The values of p_{eff} and θ for $YBa_2Cu_3O_{7-\delta}$ were $0.69\mu_B$ and -8.5 K respectively. For $(Y_{0.95}Au_{0.05})Ba_2Cu_3O_{7-\delta}$ p_{eff} and θ were $0.87\mu_B$ and $+13.4$ K and for $(Y_{0.92}Au_{0.08})Ba_2Cu_3O_{7-\delta}$ $1.06\mu_B$ and $+27.8$ K respectively. χ_0 values decrease with gold concentration. The correction for core diamagnetism was taken into account in these calculations.

Infrared absorption spectra at room temperature of the $(Y_{1-x}Au_x)Ba_2Cu_3O_{7-\delta}$ samples for different gold concentrations x are shown in Fig. 10. Fig. 10(a) concerns the oxygenated samples which are orthorhombic superconductors and Fig. 10(b) concerns the deoxygenated samples which are tetragonal semiconductors. A striking difference between (a) and (b) spectra is seen: the (a) spectra are almost featureless in contrast to a rich phonon structure of the (b) spectra. This difference occurs because the large polarizability owing to free carriers masks the phonon-related structure for the superconductor samples. The only phonon mode for the (a) spectra is seen at about 590 cm^{-1}. Its intensity is greater for gold substituted samples. The mode is

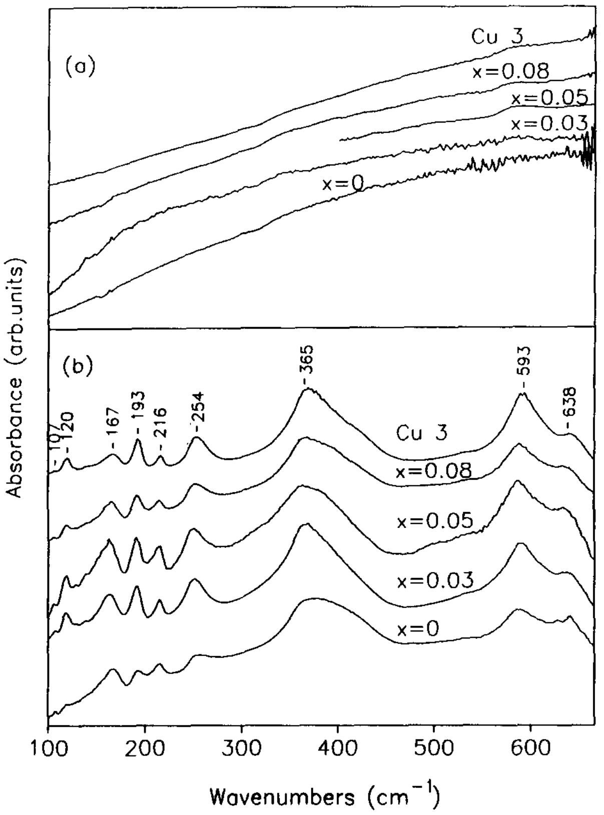

Fig. 10. Infrared absorption spectra for $(Y_{1-x}Au_x)Ba_2Cu_3O_{7-\delta}$ samples measured at room temperature. (a) and (b) concern the oxygenated and deoxygenated samples respectively. Spectra marked Cu 3 are for the $YBa_2(Cu_{0.97}Au_{0.03})_3O_{7-\delta}$ sample.

very diffuse, nonetheless no frequency shift with x can be observed.

For the (b) spectra almost all infrared active phonons are seen [18,19]. No systematic change in phonon frequencies is observed. The most pronounced difference under gold substitution is an increased intensity of the 120 cm^{-1} mode usually assigned to the Eu translation of Ba [19].

The results in Fig. 10(a) can be compared with those obtained by other authors [20] for Fe and Co substituted $YBa_2Cu_3O_{7-\delta}$. While substitution by Fe has only a minor effect on the 590 cm^{-1} mode, substitution by Co softens this mode by about 35 cm^{-1}. Both dopants are known to substitute for Cu(1), but Fe substitutes additionally for Cu(2). This mode is most often classified as B_{1u} representing in-phase axial vibration of O(4) ions about Cu(1) with a smaller axial motion of the O(1) on either side of the Cu(1). It is nearly certain that this mode is the same mode as that studied by Kuzmany et al. [21] as a function of oxygen depletion δ. This mode dominates the spectrum for the oxidized sample but is fully absent for the deoxygenated one. The mode shows a strong softening up to 50 cm^{-1} with increasing δ. It was assigned to Cu(1)–O(1) vibration. Even taking into account both above mentioned assignments it is still not clear why Co and Au substitutions behave so differently. Moreover, it was shown [22] that the suppression of superconductivity by Co substitution and oxygen depletion are in the same way correlated with Raman shift.

The intensive 590 cm^{-1} mode for deoxygenated sample seen in Fig. 10(b) is assigned to the Cu(2)–O(2,3) stretching vibration [18] and only incidentally [21] shows the same frequency as the mode from Fig. 10(a).

Two spectra of the $YBa_2(Cu_{0.97}Au_{0.03})_3O_{7-\delta}$ sample, marked Cu 3, are included also in Fig. 10. No difference with respect to previously described spectra can be seen in agreement with the statement that gold always goes into the Cu(1) chain positions.

4. Discussion of magnetic properties. Problem of magnetic impurities

In this part we discuss the problem of gold influence on magnetic properties. First of all let us take into account the result of Welp et al. [10] who observed that gold impurities do not influence the normal state susceptibility of a single crystal of $YBa_2Cu_3O_{7-\delta}$ grown in a gold crucible. This points to the fact that ion exchange takes place between the $YBa_2Cu_3O_{7-\delta}$ sample and the crucible, i.e. copper diffuses into the crucible. Thus, the crystal structure with 8 at.% of gold in chain positions seems to be more energetically stable. Let us recall that the orthorhombic structure is maintained with Au substitution. It is possible that gold so changes energetic relations, that in the case of yttrium deficiency, copper is expelled by gold from the chain to other positions in the lattice. These extra copper ions can be responsible for the change in magnetic susceptibility. At the same time the possibility of an appearance of paramagnetic Au^{3+}-ions can be disregarded here (based on the above mentioned results of Welp et al.). Besides, paramagnetic Au^{3+} were not reported, although the possibility was pointed out by Goodenough [23].

Magnetic behaviour seen in Fig. 9 can also be caused by magnetic impurities. Let us assume, based on the Mössbauer results, that all the gold was incorporated into the structure (in Cu(1) positions). Because of the yttrium deficiency the extra Ba and Cu atoms could precipitate either as compound $BaCu_2O_2$ or $BaCuO_2$ and CuO. The last two compounds should appear simultaneously (as in the case of $(Y_{0.95}Ag_{0.05})Ba_2Cu_3O_{7-\delta}$; see above). Copper in $BaCu_2O_2$ has the valence 1+ and is nonmagnetic, so probable magnetic impurities could be $BaCuO_2$ and CuO. CuO is an antiferromagnet with Néel temperature $T_N = 230$ K, with decreasing susceptibility below T_N [24]. $BaCuO_2$ is a paramagnet [25] and it could be mainly responsible for the increased values of χ, at least for greater Au concentrations. Let us take the case of $(Y_{0.92}Au_{0.08})Ba_2Cu_3O_{7-\delta}$ and estimate the susceptibility contribution $\Delta\chi$ at room temperature coming from precipitated $BaCuO_2$ and CuO. For a 1 g sample we have 0.055 g of $BaCuO_2$ and 0.02 g of CuO. Taking susceptibility values from the paper of Twin et al. [26] we obtain $\Delta\chi \approx 3.8 \times 10^{-7}$ emu g^{-1}, which is too small a value to account for the increased χ values of gold doped samples. Moreover, it follows from the paper of Kubo et al. [27] that χ of $BaCuO_2$ increases by about 40% after keeping in argon at 500 °C. So, at least the $BaCuO_2$ impurity can not be responsible for the observed magnetic behaviour of our samples.

If we, however, assume that no impurities precipitated, increased χ values for superconducting samples could origin from Cu^{2+}-ions which, expelled from chains by gold, locate themselves in vacancy positions of the lattice. Their contribution to magnetic moment $x \times \mu_B$ is in good agreement with low temperature magnetization data presented in Fig. 7.

In the process of oxygen depletion the three different coordinations of Cu(1) are possible i.e. 4, 3 or 2 oxygen neighbours with formal valencies 3+, 2+ or 1+ respectively. Only Cu^{2+} with 3 neighbours is magnetic. Concerning gold, its coordination can be only plane-square or linear. So transition from Au^{3+} to Au^{1+} (assuming that gold is located in chain positions) should be associated with the appearance of two Cu^{2+}-ions. Thus, Au substitution can increase susceptibility of nonsuperconducting samples also. Unexplained is only susceptibility drop after deoxygenation. It is worth recalling that for non substituted $YBa_2Cu_3O_{7-\delta}$ such effect, but to a lower degree was also observed [16,28].

5. Conclusions

In conclusion we state that gold added to $YBa_2Cu_3O_{7-\delta}$, substitutes for Cu in the chain positions. The samples with nominal compositions $(Y_{0.95}Au_{0.05})Ba_2Cu_3O_{7-\delta}$, i.e. with yttrium deficiency, are very homogeneous and show improved certain superconducting characteristics as compared with $YBa_2(Cu_{0.97}Au_{0.03})_3O_{7-\delta}$ and even with gold free $YBa_2Cu_3O_{7-\delta}$. We conclude also that the extra copper ions are expelled by gold to vacant positions in the lattice, probably in the yttrium plane. These extra copper ions contribute to the observed paramagnetism. No considerable T_c enhancement was confirmed. No remarkable changes in phonon spectra were observed with gold substitution.

Acknowledgements

Z.T. would like to thank K. Wojciechowski for his help at the initial stage of this work. The authors are very much indebted to J. Jedlinski from the Joint Center for Chemical Analysis and Structural Research at Jagellonian University for performing the SEM analysis. The work has been partially supported by the State Committee for Scientific Research in Poland with Grant 2-0083-91-01.

References

[1] J.J. Lin, T.-M. Chen and Y.F. Chen, *Solid State Commun, 76* (1990) 1285; Anup K. Gangopadhyay and T.O. Mason, *Physica C, 178* (1991) 64.

[2] M.Z. Cieplak, G. Xiao, C.L. Chien, A. Bakhshai, D. Artymowicz, W. Bryden, J.K. Stalick and J.J. Rhyne, *Phys. Rev. B, 42* (1990) 6200.

[3] M. Eibschütz, M.E. Lines, W.M. Reiff, B. van Dover, J.V. Waszczak, S. Zahurak and R.J. Felder, *Appl. Phys. Lett., 62* (1993) 1827.

[4] J.L. Tallon and N.E. Flower, *Physica C, 204* (1993) 237.

[5] D. Veretnik and S. Reich, *Physica C, 223* (1994) 227.

[6] C. Thomsen, B. Friedl, M. Cieplak and M. Cardona, *Solid State Commun., 78* (1991) 727; K.F. McCarty, J.Z. Liu, Y.X. Jia, R.N. Shelton and H.B. Radousky, *Physica C, 192* (1992) 331.

[7] R. Gotszalk and M. Lisowski, *Rev. Sci. Instrum., 58* (1987) 1771.

[8] J.C. Picoche, M. Guillot and A. Marchand, *Physica B, 155* (1989) 407.

[9] A.F. Hepp, J.R. Gaier, J.J. Pouch and P.D. Hambourger, *J. Solid State Chem., 74* (1988) 433.

[10] U. Welp, S. Fleshler, W.K. Kwok, J. Downey, G.W. Crabtree, H. Claus, A. Erb and G. Müller-Vogt, *Phys. Rev., 47* (1993) 12 369.

[11] P.W. Anderson and Z. Zou, *Phys. Rev. Lett., 60* (1988) 132.

[12] L.G. Aslamazow and A.I. Larkin, *Phys. Lett. A, 26* (1968) 238.

[13] M.P. Fontana, C. Paracchini, C. Paris De Renzi, P. Poddini, F. Licci and F.C. Matacotta, *Solid State Commun., 69* (1989) 621.

[14] A. Gauzzi, *Europhys. Lett., 21* (1993) 207; A. Gauzzi and D. Pavuna, *J. Alloys Comp., 195* (1993) 647.

[15] C.P. Bean, *Rev. Mod. Phys., 36* (1964) 31.

[16] G. Triscone, J.-Y. Genoud, T. Graf, A. Junod and A. Muller, *J. Alloys Comp., 195* (1993) 351.

[17] H. Claus, S. Yang, H.K. Viswanathan, G.W. Crabtree, J.W. Downey and B.W. Veal, *Physica C, 213* (1993) 185.

[18] G. Burns, F.H. Dacol, P. Freitas, T.S. Plaskett and W. König, *Solid State Commun., 64* (1987) 471.

[19] M.K. Crawford, G. Burns and F. Holtzberg, *Solid State Commun., 70* (1989) 557.

[20] B. Roughani, L.C. Sengupta, S. Sundaram and W.C.H. Joiner, *Z. Phys. B, 86* (1992) 3.

[21] H. Kuzmany, M. Matus, E. Faulques, S. Pekker, Gy. Hutiray, E. Zsoldos and L. Mihaly, *Solid State Commun., 65* (1988) 1343.

[22] L. Börjesson, L. Van Hong, M. Käll, M. Kakihana and P. Berastegui, *J. Alloys Comp., 195* (1993) 363.

[23] J.B. Goodenough, *Magnetism and the Chemical Bond*, John Wiley, 1963.

[24] K. Muraleedharan, C.K. Subramaniam, N. Venkataramani, T.K. Gundu Rao, C.M. Srivastava, V. Sankaranarayanan and R. Srinivasan, *Solid State Commun., 76* (1990) 727.

[25] R. Troć, J. Janicki, A. Zygmunt, H. Drulis and A. Niedźwiedź, *Physica B, 193* (1994) 1.

[26] A.J. Twin, J.S. Abel and I.R. Harris, *J. Less-Common Met., 164/165* (1990) 1136.

[27] Y. Kubo, Y. Shimakawa, T. Manako and H. Igarashi, *Phys. Rev. B, 43* (1991) 7875.

[28] Y. Nakazawa and M. Ishikawa, *Physica C, 158* (1989) 381.